An Eddifying Parsons Model

BAYLOR FOX-KEMPER

Cooperative Institute for Research in Environmental Sciences, and Department of Atmospheric and Oceanic Sciences, University of Colorado, Boulder, Colorado

RAFFAELE FERRARI

Department of Earth, Atmospheric and Planetary Sciences, Massachusetts Institute of Technology, Cambridge, Massachusetts

ABSTRACT

The time-mean effects of eddies are studied in a model based on the Parsons–Veronis–Huang–Flierl models of the wind-driven gyre. Much of the analysis used for the steady solutions carries over if the model is cast in terms of the thickness-weighted mean velocity, because then mass transport is nondivergent in the absence of diabatic forcing. The model exemplifies the use of residual mean theory to simplify analysis.

A result of the analysis is a boundary layer width in the case of a rapid upper-layer flow and weak lower-layer flow. This boundary layer width is comparable to an eddy mixing length when the typical eddy velocity is taken to be the long Rossby wave phase speed.

Further analysis of the model illustrates important aspects of eddy behavior, model sensitivity to eddy fluxes, and model sensitivity to frictional parameters.

1. Introduction

The ubiquitous mesoscale eddies in the ocean affect the transport and structure of tracers: salt, potential temperature, potential density, and potential vorticity (PV). The turbulent character of these eddies makes for few tractable observational, analytical, and numerical approaches. Formal mathematical treatments of eddy fluxes have revealed that careful manipulation of the definition of an eddy may provide advantages in capturing the eddy–mean flow interaction. The Transformed Eulerian Mean (TEM: e.g., Andrews et al. 1987; Vallis 2006) and Generalized Lagrangian Mean (GLM; Andrews and McIntyre 1978) frameworks are two examples.

Here the temporal residual mean formulation (TRM; McDougall and McIntosh 2001) is used to formulate a model consistent with the mean density structure of the ocean while retaining some important effects of time-dependent eddies. In an isopycnal-coordinate model, the TRM velocity is simply the thickness-weighted mean velocity, and the layer mass and tracer transports are natural. The TRM approach has been used successfully to study eddy–mean flow interactions in the atmosphere (Andrews et al. 1987). Here we show that similar advantages arise in the study of gyre circulations in enclosed domains. In particular we use the TRM formalism to include eddy feedbacks in models akin to Parsons (1969) and later extensions by other investigators.

Unlike much of the recent literature, this paper does not provide detailed maps of eddy diffusivities or viscosities: instead the TRM Parsons model compellingly illustrates the roles of eddies in a gyre circulation. In the TRM formulation, eddy effects appear as a force in the momentum equations—a fact extensively exploited here and in many atmospheric eddy–mean flow interaction studies. It is shown that eddies transfer momentum downward in the ocean interior and buoyancy poleward in the ocean mixed layer. The TRM Sverdrup relation is simply modified in the presence of eddies. The next section introduces the Parsons model and subsequent sections discuss impacts of eddies on the resulting ocean circulation.

Corresponding author address: Baylor Fox-Kemper, CIRES, University of Colorado, 216 UCB, Attn: Baylor Fox-Kemper, Boulder, CO 80309-0216.
E-mail: bfk@colorado.edu

2. Eddy–mean flow interaction in layered models

We consider a layered, rigid-lid, shallow-water, Boussinesq flow on a β plane:

$$\frac{\partial \mathbf{u}_i}{\partial t} + (\mathbf{f} + \boldsymbol{\zeta}_i) \times \mathbf{u}_i = -\nabla \mathcal{B}_i + \mathcal{F}_i, \tag{1}$$

$$\frac{\partial h_i}{\partial t} + \nabla \cdot h_i \mathbf{u}_i = w_{i+} - w_{i-}. \tag{2}$$

The upper layer is $i = 1$, and the ith layer has depth h_i, horizontal velocity $\mathbf{u}_i$, and vertical planetary ($\mathbf{f} = f_0 \mathbf{z} + \beta y \mathbf{z}$) and relative ($\nabla \times \mathbf{u}_i \equiv \boldsymbol{\zeta}_i$) vorticity. The ∇ operates within a layer along two dimensions. Wind stress and frictional forces are combined in $\mathcal{F}_i$. The possibility of cross-isopycnal flow into each layer from above (w_{i-}) or below (w_{i+}) is retained.

The Bernoulli function $\mathcal{B}_i$ is given by

$$\mathcal{B}_i \equiv \mathcal{M}_i + \frac{1}{2} \mathbf{u}_i \cdot \mathbf{u}_i,$$

with the Montgomery potential, $\mathcal{M}_i$, given by

$$\mathcal{M}_i = g \frac{\rho_{i+1} - \rho_i}{\rho_0} \sum_{j=1}^{i} h_j + \mathcal{M}_{i+1}.$$

For a two-layer model the Montgomery potential reduces to $\mathcal{M}_1 = g' h_1 + \mathcal{M}_2$, where g' is the reduced gravity [$g' \equiv g(\rho_2 - \rho_1)/\rho_0$]. The total depth is fixed at $h_1 + h_2 = H$.

Steady solutions to (1)–(2) or very similar equations are common (Parsons 1969; Veronis 1973, 1976, 1978; Pedlosky 1987; Huang and Flierl 1987; Huang 1987a,b, 1988; Godfrey 1989; Nurser and Williams 1990). Here we set up and solve the time mean of these equations, including treatment of eddy fluxes. The time mean of (1)–(2) is

$$(\mathbf{f} + \overline{\boldsymbol{\zeta}}_i) \times \overline{\mathbf{u}}_i = -\nabla \overline{\mathcal{B}}_i - \nabla \overline{K}_i + \overline{\mathcal{F}}_i - \overline{\boldsymbol{\zeta}_i' \times \mathbf{u}_i'},$$

$$\nabla \cdot \overline{h_i} \overline{\mathbf{u}}_i = \overline{w}_{i+} - \overline{w}_{i-} - \nabla \cdot \overline{h_i' \mathbf{u}_i'},$$

$$\overline{\mathcal{B}}_i \equiv \overline{\mathcal{M}_i} + \frac{1}{2} \overline{\mathbf{u}}_i \cdot \overline{\mathbf{u}}_i, \quad \overline{K}_i \equiv \frac{1}{2} \overline{\mathbf{u}_i' \cdot \mathbf{u}_i'}.$$

Overbars denote averages and primes denote perturbations therefrom.[1]

The time averaging results in eddy fluxes both in the momentum and thickness equations. Gent and McWilliams (1990) suggest that the thickness fluxes are likely to be downgradient, but momentum fluxes remain

problematic. To address this issue, a rearrangement simplifies

$$(\mathbf{f} + \overline{\boldsymbol{\zeta}}_i) \times \frac{\overline{h_i \mathbf{u}_i}}{\overline{h_i}} = -\nabla \overline{\mathcal{B}}_i - \nabla \overline{K}_i + \overline{\mathcal{F}}_i$$

$$- \left[\overline{\boldsymbol{\zeta}_i' \times \mathbf{u}_i'} - (\mathbf{f} + \overline{\boldsymbol{\zeta}}_i) \times \frac{\overline{h_i' \mathbf{u}_i'}}{\overline{h_i}} \right],$$

$$\nabla \cdot \overline{h_i} \frac{\overline{h_i \mathbf{u}_i}}{\overline{h_i}} = \overline{w}_{i+} - \overline{w}_{i-}. \tag{3}$$

If one uses the thickness-weighted mean velocity $\overline{\mathbf{u}}_i^{\dagger}$ as the prognostic variable, the eddy fluxes cluster in the momentum equation:

$$\overline{\mathbf{u}}_i^{\dagger} \equiv \frac{\overline{h_i \mathbf{u}_i}}{\overline{h_i}}, \tag{4}$$

$$(\mathbf{f} + \overline{\boldsymbol{\zeta}}_i) \times \overline{\mathbf{u}}_i^{\dagger} = -\nabla \overline{\mathcal{B}}_i + \overline{\mathcal{F}}_i + \overline{\mathcal{E}}_i, \tag{5}$$

$$\nabla \cdot \overline{h_i} \overline{\mathbf{u}}_i^{\dagger} = \overline{w}_{i+} - \overline{w}_{i-},$$

$$\overline{\mathcal{E}}_i \equiv -\nabla \overline{K}_i - \left[\overline{\boldsymbol{\zeta}_i' \times \mathbf{u}_i'} - (\mathbf{f} + \overline{\boldsymbol{\zeta}}_i) \times \frac{\overline{h_i' \mathbf{u}_i'}}{\overline{h_i}} \right]. \tag{6}$$

The thickness-weighted mean velocity $\overline{\mathbf{u}}_i^{\dagger}$ is the sum of the Eulerian mean velocity[2] and the bolus velocity $\overline{\mathbf{u}}_i^*$:

$$\overline{\mathbf{u}}_i^* \equiv \frac{\overline{h_i' \mathbf{u}_i'}}{\overline{h_i}}, \tag{7}$$

$$\overline{h_i \mathbf{u}_i} = \overline{h_i} \overline{\mathbf{u}}_i + \overline{h_i' \mathbf{u}_i'}, \tag{8}$$

$$\overline{\mathbf{u}}_i^{\dagger} = \overline{\mathbf{u}}_i + \overline{\mathbf{u}}_i^*. \tag{9}$$

Equations (5)–(6) are identical to the steady form of (1)–(2), except the velocity in (5)–(6) is the thickness-weighted mean velocity[3] and the eddy terms collected in $\overline{\mathcal{E}}_i$ add to the friction $\overline{\mathcal{F}}_i$. The mean flow remains arbitrarily inertial and nonlinear ($f \sim \overline{\zeta}$, $\Delta \overline{h} \sim \overline{h}$), and a suitable closure for $\overline{\mathcal{E}}_i$ makes (5)–(6) useful for numerical simulation (e.g., Wardle and Marshall 2000; Ferreira and Marshall 2006).

For small perturbations ($\zeta' \ll \overline{\zeta}$, $h' \ll \overline{h}$), $\overline{\mathcal{E}}_i$ is simplified by noting that Eqs. (1)–(2) materially conserve potential vorticity in the form $P_i = (f + \zeta_i)/h_i$, and that

---

[1] Reynolds averaging is assumed, so $\overline{\overline{\cdot}} \equiv \overline{\cdot}$ and $\overline{\cdot'} \equiv 0$.

[2] This is the Eulerian mean velocity following a fixed location in density coordinates, not z coordinates (see McDougall and McIntosh 2001 for discussion).

[3] Note that the velocity contained in $\overline{\mathcal{B}}_i$ is Eulerian, however. At low Rossby number, $\overline{\mathcal{B}}_i \approx \overline{\mathcal{M}}_i$ in both cases.

$$\hat{\mathbf{z}} \times \overline{P_i' \mathbf{u}_i'} \equiv \overline{\left(\frac{\mathbf{f} + \boldsymbol{\zeta}_i}{h_i}\right)' \times \mathbf{u}_i'}$$

$$\approx \frac{\overline{\boldsymbol{\zeta}_i' \times \mathbf{u}_i'}}{\overline{h}_i} - \frac{\mathbf{f} + \overline{\boldsymbol{\zeta}}_i}{\overline{h}_i} \times \frac{\overline{h_i' \mathbf{u}_i'}}{\overline{h}_i}, \qquad (10)$$

$$\overline{\boldsymbol{\mathcal{E}}}_i \approx -\boldsymbol{\nabla} \overline{K}_i - \overline{h}_i \hat{\mathbf{z}} \times \overline{P_i' \mathbf{u}_i'}.$$

Thus, the leading-order eddy terms are a gradient of eddy kinetic energy and an eddy PV flux. The appearance of the PV flux in the momentum budget is a central result of residual mean theory. Often oceanographic TRM literature focuses on simplifying the thickness budget to (6), but providing an interpretation of the eddy fluxes in the momentum Eq. (5) is equally significant.

A broad eddy closure

We now consider a class of possible closures for $\overline{\boldsymbol{\mathcal{E}}}_i$. The largest eddies dominate eddy transport, and they are typically larger than the deformation radius because of the inverse energy cascade as seen in models (Arbic et al. 2007) and observations (Stammer 1998; Scott and Wang 2005). Under these conditions, the eddy kinetic energy gradient and relative vorticity flux play a secondary role, so

$$\overline{\boldsymbol{\mathcal{E}}}_i \approx -\overline{h}_i \hat{\mathbf{z}} \times \overline{P_i' \mathbf{u}_i'}. \qquad (11)$$

The eddy forcing is the flux of PV, a materially conserved quantity. Mixing length arguments suggest that the fluxes of tracers tend down their mean gradient. Hence a plausible closure for $\overline{\boldsymbol{\mathcal{E}}}_i$ is

$$\overline{P_i' \mathbf{u}_i'} \approx -\kappa_i \mathbf{A} \cdot \boldsymbol{\nabla} \overline{P}, \qquad (12)$$

with $\mathbf{A}$ as a spatially varying symmetric[4] tensor with $O(1)$ eigenvalues so that the magnitude of eddy effects is carried by κ_i.

The simplest closure consistent with (12) has κ_i constant and $\mathbf{A}$ as the identity matrix representing isotropic PV mixing:

$$\overline{P_i' \mathbf{u}_i'} \approx -\kappa_i \boldsymbol{\nabla} \frac{(\mathbf{f} + \overline{\boldsymbol{\zeta}}_i) \cdot \hat{\mathbf{z}}}{\overline{h}_i}. \qquad (13)$$

Alternatively, Gent and McWilliams (1990) argue that the release of available potential energy by eddies supports downgradient thickness fluxes, resulting in PV fluxes given by

$$\overline{P_i' \mathbf{u}_i'} \approx \kappa_i \frac{(\mathbf{f} + \overline{\boldsymbol{\zeta}}_i) \cdot \hat{\mathbf{z}} \, \boldsymbol{\nabla} \overline{h}_i}{\overline{h}_i} \approx -\kappa_i (\mathbf{f} + \overline{\boldsymbol{\zeta}}_i) \cdot \hat{\mathbf{z}} \boldsymbol{\nabla} \frac{1}{\overline{h}_i}. \qquad (14)$$

Relative vorticity fluxes are neglected in (14), consistent with the Gent and McWilliams (1990) argument. Clearly, (14) differs from (13).

Finally, Killworth (1997) proposes a closure based on linear instability of the time-mean state assuming eddies larger than the deformation radius and yet smaller than the mean flow scale. The Killworth (1997) analysis finds anisotropic mixing as

$$\mathbf{A}_k \equiv \begin{bmatrix} \sin^2\theta & -\sin\theta\cos\theta \\ -\sin\theta\cos\theta & \cos^2\theta \end{bmatrix}. \qquad (15)$$

The angle θ lies between the most unstable wavenumber and the mean flow. Both κ_i and θ are functions of x, y, and t. This diffusivity and angle can be approximated from linear theory[5] or even from eddy-permitting simulations.[6]

Here the general form (12) will be carried throughout the analysis, but the solutions plotted use $\kappa = 2000 \text{ m}^2 \text{ s}^{-1}$ and $\mathbf{A}$ as the identity matrix.

3. A noninertial, adiabatic, reduced gravity solution

So far, the mean flow remains arbitrarily inertial and nonlinear ($f \sim \overline{\zeta}$, $\Delta \overline{h} \sim \overline{h}$). To proceed analytically the mean flow is restricted to small Rossby number ($f \gg \overline{\zeta}$, $\overline{\boldsymbol{\mathcal{B}}} \approx \overline{\boldsymbol{\mathcal{M}}}$). The western boundary current solution is thus limited, but analytic progress and clarity are aided. Under these assumptions only the essential eddy effects are needed. Indeed, all of the specific closures above—(13), (14), and (15)—result in the same solution.

The traditional configuration used to study gyre circulations in the ocean is one moving layer sitting over a motionless lower layer ($\overline{\mathbf{u}}_2^{\dagger} = 0$, $\overline{\boldsymbol{\mathcal{M}}}_2 = 0$) with no mass exchange between the layers ($\overline{w}_i = 0$). In this limit, (5)–(6) and closure (12) are

$$\mathbf{f} \times \overline{h}_1 \overline{\mathbf{u}}_1^{\dagger} = -g' \boldsymbol{\nabla} \frac{\overline{h}_1^2}{2} + \frac{\tau \hat{\mathbf{x}}}{\rho_0} - C_d \overline{\mathbf{u}}_1 - \kappa_1 f \mathbf{f} \times \mathbf{A} \cdot \boldsymbol{\nabla} \frac{\overline{h}_1}{f}, \qquad (16)$$

$$\boldsymbol{\nabla} \cdot \overline{h}_1 \overline{\mathbf{u}}_1^{\dagger} = 0. \qquad (17)$$

Friction $\overline{\boldsymbol{\mathcal{F}}}_i$ has been made explicit as zonal wind forcing $[\tau \hat{\mathbf{x}}/(\rho_0 \overline{h}_1)]$ and interfacial drag ($-C_d \overline{\mathbf{u}}_1/\overline{h}_1$). For simplicity,

---

[4] Rotational flux components result in an antisymmetric contribution, but can be absorbed into the bolus velocity by a judicious choice of gauge for small amplitude eddies (Plumb 1990).

[5] Killworth notes that an ensemble average of $\mathbf{A}_k$ over all angles would result in $\mathbf{A}_k$ being one-half the identity tensor.

[6] However, the numerical results of Nadiga (2008) indicate that finding θ may be a very challenging task.

τ will be a function of y only. Aside from the eddy contribution and thickness-weighted mean velocity replacing the steady velocity, (16)–(17) are identical to the equations studied by Parsons (1969) and Huang and Flierl (1987).

Introducing a mean transport streamfunction, $\overline{\Psi}_1^{\dagger}$, and nondimensionalizing following Parsons (1969) yields[7]

$$-\frac{\partial \overline{\Psi}_1^{\dagger}}{\partial y} = \overline{h}_1 \overline{u}_1^{\dagger} = \overline{h_1 u_1}, \quad \frac{\partial \overline{\Psi}_1^{\dagger}}{\partial x} = \overline{h}_1 \overline{v}_1^{\dagger} = \overline{h_1 v_1},$$

$$f\mathbf{V}\overline{\Psi}_1^{\dagger} = \mathbf{V}\frac{\overline{h}_1^2}{2} - \lambda \tau \hat{\mathbf{x}} + \epsilon_i \overline{\mathbf{u}}_1 + \epsilon_e f \mathbf{f} \times \mathbf{A} \cdot \mathbf{V}\frac{\overline{h}_1}{f}, \quad (18)$$

where f is nondimensional $[f = f_0/(\beta L) + y]$, and $\lambda = LW/g'\rho_0 H_1^2$, $\epsilon_e = \kappa_1 \beta L/g' H_1$, and $\epsilon_i = C_d/\beta LH_1$ are small numbers, roughly 5×10^{-3}, 2×10^{-3}, and 5×10^{-6}, with typical ocean values[8] based on the parameters of Holland and Rhines (1980). Holland and Rhines (1980) and Rhines and Holland (1979) study a quasigeostrophic, double-gyre simulation and address eddy effects similar to those described here.

The interfacial drag ϵ_i is tiny compared to ϵ_e, the "eddy form drag."[9] Lacking ϵ_e, Huang (1987a) uses an inflated value of $\epsilon_i \approx 10^{-3}$ and suggests that this crudely parameterizes baroclinic instability. Here, a more careful treatment of eddies is attempted. While $\epsilon_i \ll \epsilon_e$ allows neglecting ϵ_i altogether, ϵ_i will be retained for ready comparison to earlier studies.

First, we will seek a solution to the equivalent to the Huang and Flierl (1987) model, which has a fixed volume of water in the upper layer and a motionless deeper layer. Toward the end of the section, generalizations of this model will be made.

a. Interior solution

The solution in the ocean interior (i.e., where layer 1 has finite depth and is away from the western boundary

---

[7] Lengths are scaled by basin dimension L, times by $1/(\beta L)$, heights by mean upper-layer depth H_1, velocities by $|\mathbf{u}_1| = g'H_1/L^2\beta$, and wind stress by W.

[8] Typical ocean values (Holland and Rhines 1980): $L = 1000$ km, $H_1 = 1000$ m, $H = 5000$ m, $f_0 = 9.3 \cdot 10^{-5}$ s^{-1}, $\beta = 2 \times 10^{-11}$ s^{-1} m^{-1}, $\rho_0 = 1000$ kg m^{-3}, $W = 0.1$ N m^{-2}, $g' = 0.02$ m s^{-1}, and basin dimensions are $0 < x < L$, $-L < y < L$, $\tau = W \cos(\pi y/L)$, $C_b = H_2 r$, and $r = 10^{-7}$ s^{-1}. Additional parameters used here are $\kappa_1 = 2000$ m^2 s^{-1}, $C_d \approx \nu/H_1$, and $\nu = 10^{-4}$ m^2 s^{-1}.

[9] At the risk of being "obscurantist" (Warren et al. 1996), we refer to this effect as an "eddy form drag." This term is becoming traditional (Vallis 2006), and stems from the resemblance of the correlation of eddy velocity and layer thickness to the correlation of bottom velocity with bottom topography of true form drag. However, it is not a true "form drag," and does not even appear in the Eulerian mean momentum equation. Only in the thickness-weighted mean equations does it appear as a force. In this context, it will be shown to resemble an interfacial drag.

---

currents) is given by the combination of geostrophy plus the wind-driven Ekman (1905) flow,

$$f\mathbf{V}\overline{\Psi}_1^{\dagger} = \mathbf{V}\frac{\overline{h}_1^2}{2} - \lambda \tau \hat{\mathbf{x}}. \quad (19)$$

A low-order vorticity balance resembling the Sverdrup (1947) relation results from cross-differentiating (18) using $f = f_0/(\beta L) + y$:

$$\frac{\partial \overline{\Psi}_1^{\dagger}}{\partial x} = \overline{h}_1 \overline{v}_1^{\dagger} = -\lambda \frac{\partial \tau}{\partial y}. \quad (20)$$

The eddy and interfacial drag terms are negligible away from western boundary currents, $\lambda \gg \epsilon_e \gg \epsilon_i$.

The solution to (19)–(20) is

$$\overline{h}_{1,i}^2 - \overline{h}_{1,e}^2 = 2\lambda f^2(1-x)\frac{\partial(\tau/f)}{\partial y}, \quad (21)$$

$$\overline{\Psi}_{1i}^{\dagger} = (1-x)\lambda\frac{\partial \tau}{\partial y}. \quad (22)$$

The depth along the eastern boundary $\overline{h}_{1,e}$ is a constant to satisfy the absence of normal flow through the boundary. Conservation of upper-layer mass requires $\overline{h}_{1,e}$ to produce a mean value for $\overline{h}_1$ of 1. For the Holland and Rhines (1980) parameters, $\overline{h}_{1,e} = 1.003$.

b. Western boundary current

The Parsons (1969) model is exceptional among analytic solutions in that it possesses a western boundary current that can be attached to the coast (as is the Gulf Stream) or detached from the coast (as is the North Atlantic Drift). The solution for (16)–(17) is briefly described here; the reader is referred to Parsons (1969), Huang and Flierl (1987), and Nurser and Williams (1990) for a detailed presentation.

In the boundary current, streamwise and normal coordinates (s, n) are used. The normal direction is also stretched, $\xi = n/\delta$, by a small number δ related to the ratio of boundary current width to basin width—the exact expression is given below in (30). Inertial terms were neglected above for analytic progress, so consistency requires this width to be larger than the deformation radius. The momentum Eq. (18) becomes[10]

---

[10] The thickness-weighted mean has been used to approximate the interfacial drag term rather than the Eulerian mean velocity. This approximation is acceptable on the along-current velocities; both the Eulerian and thickness-weighted along-current mean velocities are geostrophic to first order.

$$\frac{f}{\delta}\frac{\partial \overline{\Psi}_1^{\dagger}}{\partial \xi} = \frac{1}{2\delta}\frac{\partial \overline{h}_1^2}{\partial \xi} - \lambda\tau\hat{\mathbf{x}}\cdot\hat{\mathbf{n}} - \frac{\epsilon_i}{\overline{h}_1}\frac{\partial \overline{\Psi}_1^{\dagger}}{\partial s}$$

$$- \epsilon_e f^2\left(\frac{\mathbf{A}_{n,s}}{\delta f}\frac{\partial \overline{h}_1}{\partial \xi} + \mathbf{A}_{s,s}\frac{\partial}{\partial s}\frac{\overline{h}_1}{f}\right), \quad (23)$$

$$f\frac{\partial \overline{\Psi}_1^{\dagger}}{\partial s} = \frac{1}{2}\frac{\partial \overline{h}_1^2}{\partial s} - \lambda\tau\hat{\mathbf{x}}\cdot\hat{\mathbf{s}} + \frac{\epsilon_i}{\delta\overline{h}_1}\frac{\partial \overline{\Psi}_1^{\dagger}}{\partial \xi}$$

$$+ \epsilon_e f^2\left(\frac{\mathbf{A}_{n,n}}{\delta f}\frac{\partial \overline{h}_1}{\partial \xi} + \mathbf{A}_{n,s}\frac{\partial}{\partial s}\frac{\overline{h}_1}{f}\right). \quad (24)$$

The nondimensionalization indicates that variations in $\overline{h}_1$ are $O(1)$, $\partial f/\partial s = O(1)$, but $\partial f/\partial \xi = O(\delta)$.

The streamwise flow in (23) is geostrophic to lowest order:

$$f\frac{\partial \overline{\Psi}_1^{\dagger}}{\partial \xi} = \frac{1}{2}\frac{\partial \overline{h}_1^2}{\partial \xi}. \quad (25)$$

Since the eddy terms are negligible in (23), both the streamwise Eulerian and thickness-weighted mean velocities are geostrophic at this order. However, (25) does not specify δ [an arbitrarily thin δ is used by Veronis (1973) and Godfrey (1989)].

The eddy parameterization determines δ. The dominant balance of (24) shows that the cross-streamflow is affected at leading order by the *cross-stream eddy transfer* or the *alongstream drag* if $\epsilon_e\mathbf{A}_{n,n} \sim \delta$ or $\epsilon_i \sim \delta$, respectively:

$$f\frac{\partial \overline{\Psi}_1^{\dagger}}{\partial s} = \frac{1}{2}\frac{\partial \overline{h}_1^2}{\partial s} + \frac{\epsilon_i}{\delta\overline{h}_1}\frac{\partial \overline{\Psi}_1^{\dagger}}{\partial \xi} + \frac{\epsilon_e f\mathbf{A}_{n,n}}{\delta}\frac{\partial \overline{h}_1}{\partial \xi}. \quad (26)$$

In (26) the difference between Eulerian and thickness-weighted mean is crucial; in the TRM momentum balance the eddy fluxes play the same role as the frictional terms do in steady solutions.

Cross-differentiating (25)–(26) forms the boundary current vorticity equation. With (25) it provides an equation for $\overline{h}_1$ alone:

$$\frac{\partial f}{\partial s}\frac{\partial \overline{\Psi}_1^{\dagger}}{\partial \xi} = -\frac{\partial}{\partial \xi}\frac{\epsilon_i}{\delta\overline{h}_1}\frac{\partial \overline{\Psi}_1^{\dagger}}{\partial \xi} - \frac{\partial}{\partial \xi}\frac{\epsilon_e f\mathbf{A}_{n,n}}{\delta}\frac{\partial \overline{h}_1}{\partial \xi},$$

$$\frac{\partial f}{\partial s}\frac{\partial \overline{h}_1^2}{\partial \xi} = -\frac{2\epsilon_i}{\delta}\frac{\partial^2 \overline{h}_1}{\partial \xi^2} - \frac{\partial}{\partial \xi}\frac{2\epsilon_e f^2\mathbf{A}_{n,n}}{\delta}\frac{\partial \overline{h}_1}{\partial \xi}. \quad (27)$$

If the eddy statistics ($\mathbf{A}_{n,n}$ and ϵ_e) can be approximated as constant across the boundary current at each location, then the solution to (27) is

$$\overline{h}_1 = \overline{h}_{1,i}\frac{1 - Be^{-(n-n_w)/\delta_b}}{1 + Be^{-(n-n_w)/\delta_b}}, \quad (28)$$

$$B = \frac{\overline{h}_{1i} - \overline{h}_{1,w}}{\overline{h}_{1,i} + \overline{h}_{1,w}}, \quad (29)$$

where $\overline{h}_{1,w}$ is the depth of the upper layer at the western boundary (or $\overline{h}_{1,w} = 0$ at an outcrop), n_w is the location of the western boundary or outcrop line, and by semigeostrophy we have $\overline{h}_{1,w}^2 = \overline{h}_{1,i}^2 - 2f\overline{\Psi}_{1,i}^{\dagger}$. The values of $\overline{h}_{1,i}$ and $\overline{\Psi}_{1,i}^{\dagger}$ to be used are the westernmost values from the interior solution (21)–(22).

Importantly, the boundary current width is

$$\delta_b = \frac{\epsilon_i + \epsilon_e f^2\mathbf{A}_{n,n}}{\overline{h}_{1,i}\dfrac{\partial f}{\partial s}}. \quad (30)$$

This width reduces to the classical forms given by Parsons (1969) and Stommel (1948), who considered only drag on a steady flow. The addition of eddies results in an eddy form drag contribution with a parametric dependence on f.

The dimensional form of δ_b is

$$\delta_b = \frac{f^2\kappa_1\mathbf{A}_{n,n}}{g'\overline{h}_{1,i}\dfrac{\partial f}{\partial s}}. \quad (31)$$

In terms of the deformation radius ($L_d = \sqrt{g'\overline{h}_{1,i}}/f$), long Rossby wave speed ($c_R = \beta L_d^2$), and mixing length approximation ($\kappa_1 = L_e U_e$), this boundary layer width is comparable to the mixing length for eddies with $U_e = c_R$, multiplied by an $O(1)$ geometric factor:

$$\delta_b = \frac{\kappa_1}{c_R}\frac{\mathbf{A}_{n,n}}{\hat{\mathbf{s}}\cdot\hat{\mathbf{y}}}. \quad (32)$$

Chelton et al. (2007) show that relevant eddy velocity scales are close to the Rossby wave speed. This width is 50 km for the typical ocean values above.[11]

A uniform solution valid in the interior and in the western boundary at the same level of approximation is derived by inserting (21) into (28):

---

[11] This width is close to the deformation radius (40 km) and depends on the assumed value of κ_1, which questions the validity of the scalings here. However, the parameters are chosen here to reproduce Holland and Rhines' (1980) values, not a clean scale separation.
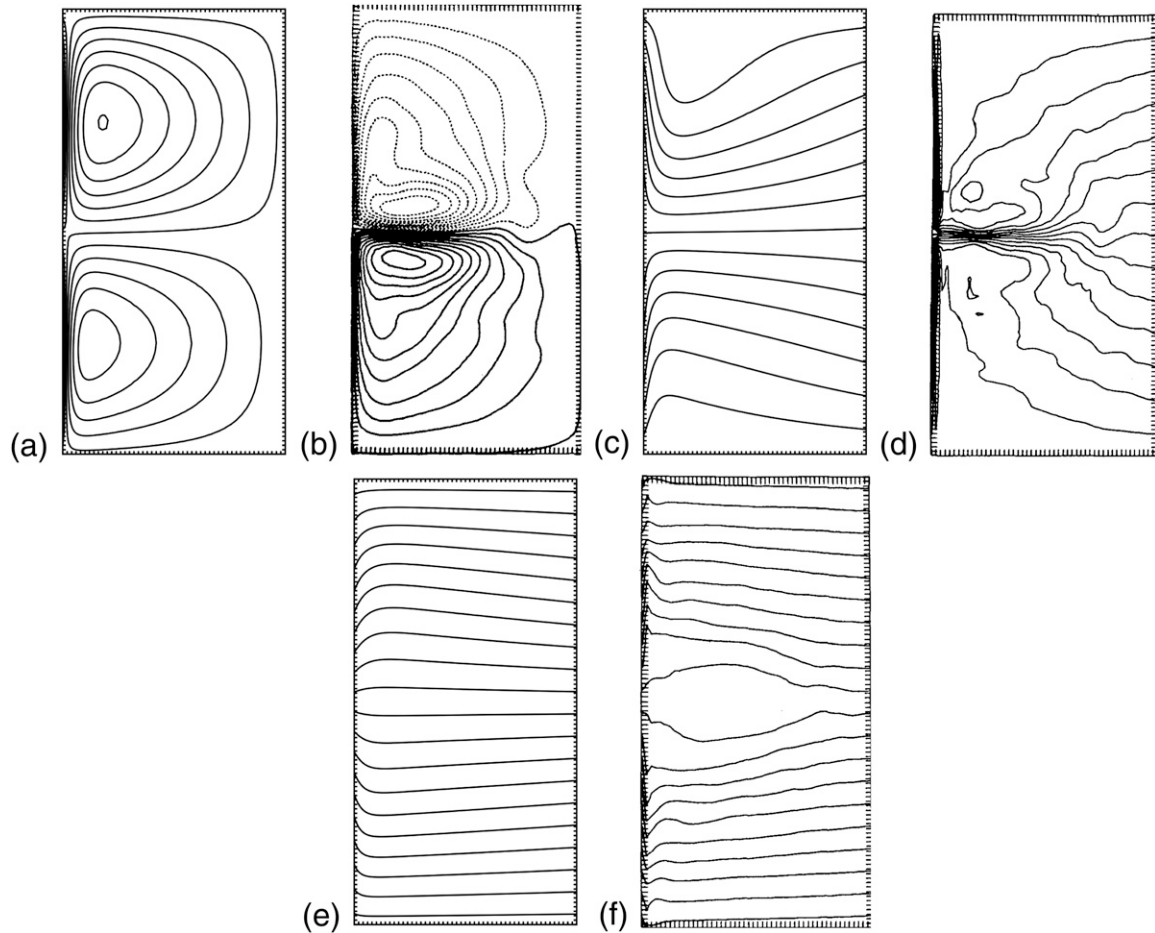
FIG. 1. Upper-layer thickness in the (a) uniform solution and (b) Holland and Rhines (1980) eddy-producing numerical solution. PV of the upper layer in the (c) uniform solution and (d) eddy-producing numerical solution. PV of the lower layer in the (e) uniform solution and (f) eddy-producing numerical solution. Contour intervals are matched.

$$\overline{h}_1 = \sqrt{\overline{h}_{1,e}^2 + 2\lambda f^2(1-x)\frac{\partial(\tau/f)}{\partial y}\frac{1-Be^{(x-x_w)\hat{\mathbf{n}}\cdot\hat{\mathbf{x}}/\delta_b}}{1+Be^{-(x-x_w)\hat{\mathbf{n}}\cdot\hat{\mathbf{x}}/\delta_b}}}.$$

$$(33)$$

Figure 1 compares the uniform solution (33) to the results of Holland and Rhines (1980). Note that the changes to layer depth are consistent with the numerical solution, and likewise the potential vorticity perturbations against the western boundary are similar in both layers. The solution reproduces the simulation results *without the introduction of an unrealistically large interfacial drag*. The boundary layer structure results from lateral eddy PV flux.

The analytic solution misses a number of features. Obviously, the recirculation gyres are missing, largely because of the neglect of advection of mean flow momentum by the mean flow (these gyres form even in steady solutions; e.g., Cessi and Ierley 1995). Further-

more, Holland and Rhines (1980) note that the eddy kinetic energy and effective eddy diffusivity are much larger in the recirculation gyres than elsewhere, implying that κ_1 should be larger there. While (27) can be used with spatially varying eddy statistics, the numerical implementation of this effect is beyond the scope of this work. PV homogenization (Rhines and Young 1982a) below the recirculation gyre area is also less effective. These missing features are expected given the assumed scale separation between the boundary layer width (31) and the deformation radius. This separation is not large for the parameters used here.

The effects of f on widening boundary layer width are minor in this simulation. The basin is small—the change in f is only two-fifths of f_0—so the error in approximating ϵ_e precludes a close comparison.

Nonetheless, the solution is sufficiently interesting to consider other flow regimes, including outcropping boundary layers and simple thermodynamic forcing (see
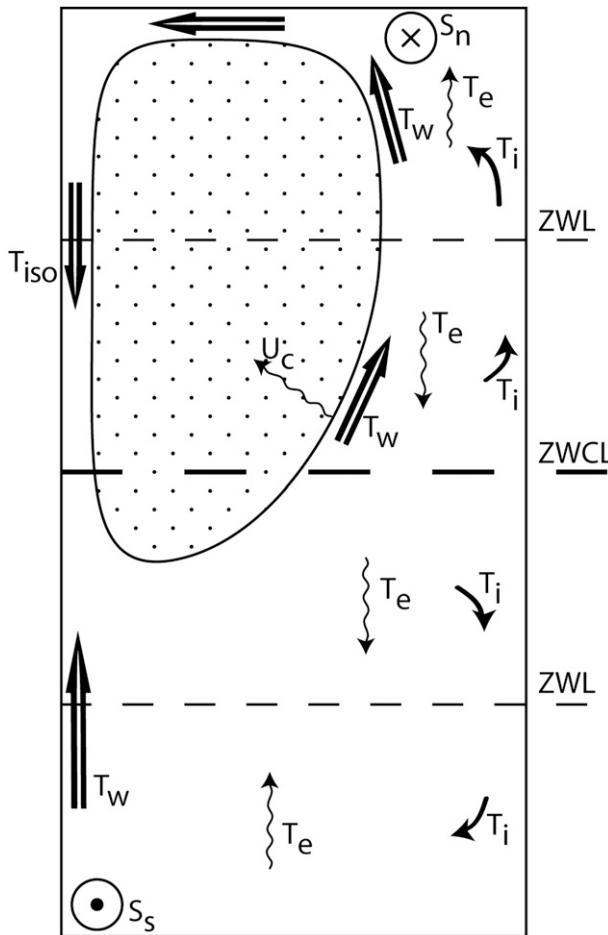
FIG. 2. The transports, sources, and sinks of the Nurser and Williams (1990) generalization of the Huang and Flierl (1987) and Veronis (1978) models. Thick double arrows are boundary currents, curvy arrows are mixed layer flows, and solid bent arrows are interior geostrophic flows. The ZWL and zero wind stress curl lines (ZWCL) are indicated.

Fig. 2). Because the boundary current is narrow and geostrophic in the along-current direction, the location of the outcrop can be estimated without a detailed eddy parameterization. Thus, all Huang and Flierl (1987) solutions immediately apply. For example, the transport along the western boundary and outcrop need not equal the interior geostrophic and Ekman flows. Huang and Flierl (1987) propose a solution of this kind, where an isolated western boundary current running along the western wall (T_{iso} in Fig. 2) is added to a western boundary current outcropping in the basin interior (T_w in Fig. 2). The streamfunction at the outcrop is different from $\overline{\Psi}_{1,e} = 0$, and is found from the net geostrophic and Ekman flow east of the outcrop,

$$\overline{\Psi}_{1,m} = -\frac{\overline{h}_{1,e}^2}{2f} + \lambda(1-x)\frac{\tau}{f}. \tag{34}$$

At the zero wind stress line (ZWL) of the subpolar gyre (see Fig. 2), this transport depends only on $\overline{h}_{1,e}$. From its value there all other transports can be determined. The critical latitude of outcrop separation y_c is found at the point where the outcrop meets the western boundary,

$$\overline{\Psi}_{1,m} = -\frac{\overline{h}_{1,e}^2}{2f_c} + \lambda\frac{\tau_c}{f_c}. \tag{35}$$

The values of f_c and τ_c are the Coriolis parameter and wind stress at y_c. The outcrop location is given by

$$x_o = 1 - \frac{\dfrac{\overline{h}_{1,e}^2}{2}(f_c - f) + \lambda f \tau_c}{\lambda \tau f_c}.$$

The eddy PV flux added here is crucial, however, in obtaining reasonable solutions. The PV flux allows reasonable boundary current width and velocity under typical oceanic parameters. The Huang and Flierl (1987) steady solution with the same parameters (except $\epsilon_e = 0$) has a boundary current 400 times thinner and velocities 400 times faster.

4. Eddy implications

Now that a solution with realistic eddy effects is complete, the remainder of this paper illustrates some of the implications.

a. An important condition on eddy fluxes

Many authors emphasize that eddies do not create momentum during baroclinic instability; they merely rearrange it. Following Killworth (1997) for the model used here, the requirement

$$0 = \sum_{i=1}^{N}\overline{h_i'\mathbf{u}_i'} \equiv \sum_{i=1}^{N}\overline{h}_i\overline{\mathbf{u}}_i^* \tag{36}$$

guarantees that the effects on depth-integrated momentum by the PV flux forcing term vanish:[12]

$$\sum_{i=1}^{N}\overline{h}_i^2\overline{P_i'\mathbf{u}_i'} = \sum_{i=1}^{N}\overline{h}_i^2\overline{P}_i\frac{\overline{P_i'\mathbf{u}_i'}}{\overline{P}_i} = \sum_{i=1}^{N}\overline{h}_i^2\overline{P}_i\frac{\overline{h_i'\mathbf{u}_i'}}{\overline{h}_i},$$

$$= \sum_{i=1}^{N}f\overline{h_i'\mathbf{u}_i'} = 0.$$

Killworth (1997) demonstrates that linear instabilities automatically obey this constraint. Marshall (1981) shows

---

[12] This is assuming that relative vorticity fluxes are neglected, consistent with eddies being larger than the deformation radius.

that the constraint persists even at modest Rossby numbers in a channel. Similar constraints are studied elsewhere (Green 1970; Held 1975; Treguier et al. 1997).

Even in a simple two-layer rigid lid model neglecting relative vorticity gradients as above, but with a moving lower layer, (36) is a difficult constraint to satisfy;

$$\kappa_1 f \mathbf{A} \cdot \nabla \frac{\overline{h}_1}{f} = \overline{h_1 \mathbf{u}_1^*} = -\overline{h_2 \mathbf{u}_2^*} = \kappa_2 f \mathbf{A} \cdot \nabla \frac{\overline{h}_2}{f},$$

$$\overline{h}_2 = H - \overline{h}_1, \quad \nabla H = 0,$$

gives the constraint $(\kappa_1 - \kappa_2) f \mathbf{A} \cdot \nabla (\overline{h}_1 / f) = \kappa_2 \mathbf{A} \cdot (0, \beta)$. Thus, even if κ_1 and $\mathbf{A}$ were simple, κ_2 would have nontrivial spatial variation.

b. A weakly moving lower layer

Instead of specifying κ_2 in this simple model, one can just impose (36) to specify the lower-layer eddy fluxes. A complete solution of this second-order problem is beyond the scope of this paper, but a magnitude estimate of the lower-layer flow in the Holland and Rhines (1980) subcritical case (i.e., no outcropping) illustrates the power of residual mean gyre dynamics. At leading order $\overline{\mathbf{u}}_1^*$ is nonzero, while $\overline{\mathbf{u}}_2 = \overline{\mathbf{u}}_2^* = 0$. At the next order, the *nonvanishing* lower-layer solution will experience upper-layer forcing via eddy form drag from (36) as well as bottom drag:

$$f \nabla \overline{\Psi}_2^\dagger = \overline{h}_2 \nabla \mathcal{M}_2 + \epsilon_b \overline{\mathbf{u}}_2 - \epsilon_2 f \mathbf{f} \times \mathbf{A} \cdot \nabla \frac{\overline{h}_1}{f}, \quad (37)$$

$$\frac{\partial \overline{\Psi}_2^\dagger}{\partial x} = J(\overline{h}_2, \mathcal{M}_2) + \mathrm{curl}\left(\epsilon_b \overline{\mathbf{u}}_2 - \epsilon_e f \mathbf{f} \times \mathbf{A} \cdot \nabla \frac{\overline{h}_1}{f} \right). \quad (38)$$

The variable $\epsilon_b = C_b / \beta L H_2$ is the nondimensional bottom drag coefficient, which is 5×10^{-3} in Holland and Rhines (1980).

Holland and Rhines (1980) discuss a "turbulent" Sverdrup balance in their model, where the ϵ_e term acts as a wind stress and presumably balances advection of planetary vorticity, $\partial \overline{\Psi}_2^\dagger / \partial x$. This balance requires

$$\overline{v}_2^\dagger \sim \frac{\epsilon_e \partial \overline{h}_1}{\overline{h}_2 \partial x}, \quad \text{or} \quad \overline{v}_2^\dagger \sim \frac{\epsilon_e f}{\overline{h}_2} \frac{\partial^2 \overline{h}_1}{\partial x^2}. \quad (39)$$

In dimensional units, this is

$$\overline{v}_2^\dagger \sim \frac{\kappa_1 f}{g' H_2} \overline{v}_1^\dagger = 2 \times 10^{-3} \overline{v}_1^\dagger, \quad \text{or} \quad (40)$$

$$\overline{v}_2^\dagger \sim \frac{\kappa_1 f^2}{g' H_2 \beta L^2} \frac{\partial \overline{v}_1^\dagger}{dx}. \quad (41)$$

The first estimate is orders of magnitude smaller than the roughly one-fifth velocity ratio found by Holland and Rhines (1980), and the second is even smaller. Thus, the vorticity balance in (38) likely involves the baroclinic forcing term $J(\overline{h}_2, \mathcal{M}_2)$ that is missing from the usual Sverdrup balance by integration (see section 4d).

In contrast, if the vorticity Eq. (38) is *integrated over a closed streamline*, Rhines and Young (1982b) show that a balance between bottom drag[13] and the interfacial forcing term—in this case the eddy forcing—results. Over repeated loops around the closed contour the circulation is determined. So,

$$\overline{v}_2^\dagger \sim \frac{\epsilon_e}{\epsilon_b} \overline{v}_1^\dagger \approx \frac{2}{5} \overline{v}_1^\dagger, \quad (42)$$

which agrees roughly with the simulations of Holland and Rhines (1980) and the idealized midocean gyre of Rhines and Young (1982b). Furthermore, Holland and Rhines (1980) found this balance to be the dominant lower-layer vorticity balance when integrated within streamlines.

Thus, the amount of vertical shear balances downward eddy form drag and bottom friction to determine the equilibrated flow. Recent equilibrated quasigeostrophic turbulence simulations agree (Arbic and Flierl 2004; Thompson and Young 2006).

c. Diabatic eddies in the mixed layer

Pedlosky (1987) adds a diabatic transport in a model similar to the Parsons (1969) model by capping it with an Ekman flow within an independent surface mixed layer. The Ekman flow provides pumping to the geostrophic interior and is allowed to change its density as it moves, resembling that of the Luyten et al. (1983) model. The resulting model does not have a separated western boundary current. By contrast, the adiabatic model above combines the Ekman and geostrophic flows in the upper layer to cause separation in (34)–(36).

Nurser and Williams (1990) explore the thermodynamic implications of allowing the Ekman layer water to change density classes within the mixed layer (U_c in Fig. 2). Similarly, Veronis (1978) was successful in perturbing the Veronis (1973) adiabatic solution by adding flow to the western boundary currents with localized diabatic sinking near the poles (S_n in Fig. 2) and localized diabatic upwelling near the equator (S_s in Fig. 2). These authors impose heating or cooling in particular locations and infer the layer transport based on the loss or gain of fluid.

---

[13] Bottom drag magnitude is again approximated with $\overline{\mathbf{u}}_2^\dagger \sim \overline{\mathbf{u}}_2$.

Nurser and Williams (1990) consider all of the diabatic forcings in Fig. 2. The essential balance they propose is that the northward transport of light water east of the outcrop is $T_{\text{north}} = T_e + T_i + T_w$, composed of the Ekman, interior geostrophic, and western boundary transport. These flows are schematized in Fig. 2 and are determined by

$$T_e = -(x_e - x_o)\frac{\tau}{f\rho_0},$$

$$T_i = \frac{g'}{2f}[\overline{h}_{1,e}^2 - \overline{h}_{1,i}^2(x_o)] = -\frac{f}{\beta}(x_e - x)\frac{\partial}{\partial y}\frac{\tau}{f\rho_0},$$

$$T_w = \frac{g'}{2f}[\overline{h}_{1,i}^2(x_o) - \overline{h}_{1,w}^2].$$

If the Ekman transport and any additional "mixed layer" flow are allowed to be diabatic, then there must be a compensating surface buoyancy flux,

$$U_c = \left(-\frac{\tau\hat{\mathbf{y}}}{f\rho_0} + h_m\mathbf{u}_m\right) \cdot \hat{\mathbf{n}} = \frac{-\alpha Q_{\text{in}}}{C_w(\rho_2 - \rho_1)/\Delta l},$$

where Q_{in} is buoyancy forcing (scaled as a heat flux in W m^{-2} into the ocean), $\alpha \approx 2.2 \times 10^{-4}$ K^{-1} is the expansion coefficient, $C_w \approx 4000$ J kg^{-1} K^{-1} is the heat capacity of seawater, and Δl is the distance over which the cooling occurs. Under realistic cooling this thermodynamic forcing increases the separated boundary current transport and moves the location of the outcrop southeastward:

$$x_o(y)_{\text{diabatic}} - x_o(y)_{\text{adiabatic}} = \frac{f\rho_0}{\tau}\int_y^{y_0} U_c \, ds.$$

Here, $\overline{h}_1\overline{\mathbf{u}}_1^\dagger$ is the nondivergent time-mean transport. Generally, layered tracer equations take the form

$$\frac{\partial}{\partial t}h_i\phi_i + \nabla \cdot h_i\phi_i\mathbf{u}_i = 0 \qquad (43)$$

for the tracer concentration ϕ, which could be salinity, potential temperature, potential density, etc. After averaging, the upper interior layer density equation is[14]

$$\nabla \cdot \overline{h}_1\rho_1\overline{\mathbf{u}}_1^\dagger = -\rho_1\overline{w}_{1-}. \qquad (44)$$

---

[14] A term $-\nabla \cdot \overline{(\mathbf{u}_i - \overline{\mathbf{u}}_i^\dagger)[\phi_i - (\overline{h_i\phi_i}/h_i)]}$ that might appear in the mean tracer equation is addressed carefully by Dukowicz and Greatbatch (1999) and Lee (2002) for the case of general tracers. Here the tracer (potential density) is constant in each layer and this term vanishes.

As in Nurser and Williams (1990), the mass in the upper layer is diminished by entrainment into the mixed layer by $\overline{w}_{1-}$. Buoyancy forcing enters through conservation of mixed layer volume, which is affected by Ekman and mixed layer flow divergence:

$$\nabla \cdot \left(-\frac{\tau\hat{\mathbf{y}}}{f\rho_0} + h_m\mathbf{u}_m\right) = \overline{w}_{1-}. \qquad (45)$$

What is the physical basis of this mixed layer flow? Nurser and Williams (1990) do not specify, but it is directed across the mean density gradient at the outcrop so as to flatten the isopycnal slope, closes the residual circulation transport budget (44)–(45), and responds promptly to balance surface cooling events. These are characteristic behaviors of near-surface eddy fluxes, as shown by Ferrari and Plumb (2003) and Plumb and Ferrari (2005). These fluxes are cast as an eddy parameterization scheme by Ferrari et al. (2008).

d. The depth-integrated equations

Rhines and Holland (1979) and Radko and Marshall (2004) note that in numerical simulations the eddy fluxes leak away from the boundary into the interior and affect the vorticity balance there. They analyze an eddy-induced vortex stretching in addition to the Ekman wind forcing for the upper-layer vorticity balance. This section shows that TRM naturally includes this effect.

The Eulerian Sverdrup (1947) constraint is found by depth integrating and cross-differentiating the momentum equations:

$$\int_{-H}^0 \beta\overline{v} \, dz = \sum_{i=1}^N \beta\overline{v}_i\overline{h}_i = \text{curl}\left(\frac{\tau}{\rho_0}\right). \qquad (46)$$

An equivalent thickness-weighted version is

$$\sum_{i=1}^N \beta\overline{v_ih_i} = \text{curl}\left(\frac{\tau}{\rho_0}\right). \qquad (47)$$

Equations (46) and (47) are equivalent because of the constraint (36), as

$$\sum_{i=1}^N \beta(\overline{v_ih_i} - \overline{v}_i\overline{h}_i) = \beta\sum_{i=1}^N \overline{h_i'v_i'} = 0. \qquad (48)$$

However, consider the upper-layer flow over a weakly moving abyss as in section 4b. At leading order, cross-differentiation eliminates the Montgomery potential, to wit,

$$\text{curl}(\overline{h}_1\nabla\overline{\mathcal{M}}_1) = \text{curl}[\nabla(g'\overline{h}_1^2/2)] = 0.$$

It is trivial to add the eddy momentum forcing to the wind forcing in the residual mean formulation, and thus the upper-layer vorticity equation is

$$\beta \overline{h}_1 \overline{v}_1^{\dagger} = \text{curl}(\overline{h}_1 \overline{\mathcal{F}}_1 + \overline{h}_1 \overline{\mathcal{E}}_1) \neq \beta \overline{h}_1 \overline{v}_1. \qquad (49)$$

This vorticity balance will hold whether or not strong eddy forcing is present. The thickness-weighted upper-layer vorticity equation resembles the thickness-weighted Sverdrup relation (47).

Approaching the same problem in the Eulerian mean formulation, cross-differentiation of the Coriolis term leaves $\beta \overline{h}_1 \overline{v}_1$ and $f\nabla \cdot \overline{h}_1 \overline{\mathbf{u}}_1 = -f\nabla \cdot \overline{h_1' \mathbf{u}_1'}$. Thus, the upper-layer Eulerian vorticity equation is unlike the Eulerian Sverdrup relation (46). The "leaky thermocline" theory of Radko and Marshall (2004) uses a seemingly diapycnal transport $\tilde{w}_{1-}$ to account for this term:

$$\tilde{w}_{1-} = -\nabla \cdot \overline{h_1' \mathbf{u}_1'}. \qquad (50)$$

Careful diagnosis of $f\tilde{w}_{1-}$ results in a similar term[15] to curl $(\overline{h}_1 \overline{\mathcal{E}}_1)$ found trivially in (49). However, the quantity $\tilde{w}_{1-}$ is *not* an indicator of true diapycnal exchange or leakiness. For example, it is nonzero in the boundary current vorticity balance (26) despite the strictly adiabatic conditions there. In the real ocean some interior diapycnal transformation results from diffusion–mesoscale interaction, as Radko and Marshall (2004) also suggest. In TRM this latter physical effect, which produces $\overline{w}_{1-}$ in the thickness-weighted mean Eq. (3) and a corresponding vortex stretching term $f\overline{w}_{1-}$ in (49), is distinguished from the kinematic effect of $f\tilde{w}_{1-}$ that appears only if the Eulerian mean velocity is used.

Similarly, the depth-integrated momentum equations here resemble the steady Stommel (1948) model, as eddy momentum transfers from layer to layer cancel out, leaving only wind stress and bottom drag (the Antarctic Circumpolar Current has a similar depth-integrated balance as shown by Johnson and Bryden 1989). Unlike the barotropic Stommel model, vertical shear is permitted at density interfaces with a magnitude consistent with the Margules relation and controlled by the eddy form drag as in (42). Only in an eddy-resolving or eddy-parameterizing model can the shear be quantified.

e. Boundary conditions and global constraints

The treatment of eddies here is more realistic than in previous models. However, it should be noted that inertial terms are neglected by assuming that eddy and mean scales exceed the deformation radius. Relaxing

---

this constraint defies eddy parameterization, because the neglected terms (e.g., $\nabla \overline{K}_i$) are unlikely to be downgradient or local (Holland and Rhines 1980; Berloff 2005). Global constraints on the vorticity are used in the literature to indicate global inertial behavior, but $O(1)$ variations in layer depth are usually ignored (e.g., Harrison and Holland 1981; Fox-Kemper and Pedlosky 2004).

By integrating (5) around a streamline of $\overline{\Psi}_i^{\dagger}$, the only remaining nonzero terms are

$$\oint \overline{\mathcal{F}}_i \cdot d\mathbf{l} = \oint \overline{h}_i \overline{P_i' \mathbf{u}_i'} \cdot \hat{\mathbf{n}} \, ds. \qquad (51)$$

Thus, as in Fox-Kemper and Pedlosky (2004), an imbalance in wind and friction torque around the streamline (both part of $\overline{\mathcal{F}}$) may be kept in check by an outward eddy flux of potential vorticity. However, at the streamline that coincides with the boundary of the domain $\overline{P_i' \mathbf{u}_i'} \cdot \hat{\mathbf{n}} = 0$, so ultimately all of the vorticity input by the wind must be removed frictionally.

The eddy-resolving models of Berloff (2005) and Fox-Kemper (2004) reveal a layered structure of eddy fluxes near the boundary, which one expects to be true with $O(1)$ depth variations as well. The seaward boundary layer is the one parameterized here, where potential vorticity fluxes of thickness tend to flatten the isopycnals. At a deformation radius from the boundary, thickness PV fluxes are exchanged for relative vorticity PV fluxes. Finally, in a viscous sublayer, relative vorticity PV fluxes are removed from the basin frictionally.

Interestingly, the outcrop line does not behave as a rigid boundary in this regard: the eddy flux into the separated boundary current $\overline{P_i' \mathbf{u}_i'} \cdot \hat{\mathbf{n}}$ need not be zero. One layer may exchange PV with the next at the boundary, as PV impermeability (Haynes and McIntyre 1987) is easily overcome at the boundary. Indeed, the parameterization used here predicts a large flux into the outcrop where $\nabla f/\overline{h}_1$ takes a large value. This outcrop PV flux may be related to the mixed layer flow in section 4c above. Just as for heat transfer, surface diabatic effects must be involved and thermodynamic constraints must be satisfied (Marshall and Nurser 1992).

5. Conclusions and summary

A reconciliation of the residual, or thickness-weighted, mean and the traditional steady wind-driven gyre model initially studied by Parsons (1969) reveals that most of the traditional solution methods proceed with little modification. The interpretation of the solutions, however, is unfamiliar as the thickness-weighted mean velocity (not the Eulerian mean velocity) plays the role of the steady

---

[15] This is aside from relative vorticity contributions.

velocity. The thickness-weighted mean velocity appears because its transport is nondivergent even in an eddying flow, unlike the Eulerian mean. It is shown that an "eddy form drag" results from a realistic parameterization of along-isopycnal eddy fluxes of potential vorticity and plays the role of the unrealistically large interfacial friction typically found in steady models.

The boundary layer width of the upper-layer flow based on eddy statistics is found to be

$$\delta_b = \frac{\kappa}{c_R} \frac{1}{\hat{\mathbf{s}} \cdot \hat{\mathbf{y}}}, \qquad (52)$$

where c_R is the long Rossby wave phase speed, and κ is the eddy diffusivity normal to the boundary current.[16] This boundary layer width holds if κ varies, so long as the variation across the boundary current at a given location is small. Formally, this scaling was shown to hold only when it exceeds the deformation radius. This boundary layer width is comparable to an eddy mixing length scale if the typical eddy velocity is taken to be the long Rossby wave speed.

This model sheds light on the behavior of eddies in the gyre circulation. An important constraint—that eddies only rearrange and do not create momentum—is shown to be crucial to recover the traditional Sverdrup (1947) relation upon integration over the total ocean depth. However, eddies do redistribute momentum in the vertical, as shown by (49). To maintain a Sverdrup-like upper-layer vorticity equation under the effects of eddies, the thickness-weighted mean velocity may be used.

Inertia is a crucial aspect of gyre flows missing from this simple model, which was chosen primarily to illustrate, not simulate. Relatedly, the eddy parameterization here allows eddy PV fluxes through the boundary, while resolved eddies must transfer these fluxes to frictional or diffusive ones as in the second case studied by Fox-Kemper and Pedlosky (2004). Perhaps an extension including the eddy advection of eddy relative vorticity—at least for weak eddies—is possible using a similar form of eddy parameterization to that used here [see (10) and Plumb 1990]. Even so, the mean advection of mean relative vorticity usually requires numerical simulations (e.g., Cessi and Ierley 1995; Speich et al. 1995) or analytic methods beyond the treatment here (Charney 1955; Huang 1990).

REFERENCES

Andrews, D. G., and M. E. McIntyre, 1978: An exact theory of nonlinear waves on a Lagrangian-mean flow. *J. Fluid Mech.,* **89,** 609–646.

——, J. R. Holton, and C. B. Leovy, 1987: *Middle Atmosphere Dynamics.* Academic Press, 489 pp.

Arbic, B. K., and G. R. Flierl, 2004: Baroclinically unstable geostrophic turbulence in the limits of strong and weak bottom Ekman friction: Application to midocean eddies. *J. Phys. Oceanogr.,* **34,** 2257–2273.

——, ——, and R. B. Scott, 2007: Cascade inequalities for forced–dissipated geostrophic turbulence. *J. Phys. Oceanogr.,* **37,** 1470–1487.

Berloff, P., 2005: On dynamically consistent eddy fluxes. *Dyn. Atmos. Oceans,* **38,** 123–146.

Cessi, P., and G. R. Ierley, 1995: Symmetry-breaking multiple equilibria in quasigeostrophic, wind-driven flows. *J. Phys. Oceanogr.,* **25,** 1196–1205.

Charney, J. G., 1955: The Gulf Stream as an inertial boundary layer. *Proc. Natl. Acad. Sci. USA,* **41,** 731–740.

Chelton, D., M. Schlax, R. Samelson, and R. de Szoeke, 2007: Global observations of large oceanic eddies. *Geophys. Res. Lett.,* **34,** L15606, doi:10.1029/2007GL030812.

Dukowicz, J., and R. Greatbatch, 1999: The bolus velocity in the stochastic theory of ocean turbulent tracer transport. *J. Phys. Oceanogr.,* **29,** 2232–2239.

Ekman, V. W., 1905: On the influence of the earth's rotation on ocean currents. *Arkiv. Mat. Astron. Fysik.,* **2,** 1–53.

Ferrari, R., and R. A. Plumb, 2003: Residual circulation in the ocean. *Near-Boundary Processes and Their Parameterization: Proc. 'Aha Huliko'a Hawaiian Winter Workshop,* Honolulu, HI, University of Hawaii at Manoa, 219–228.

——, J. C. McWilliams, V. M. Canuto, and M. Dubovikov, 2008: Parameterization of eddy fluxes near oceanic boundaries. *J. Climate,* **21,** 2770–2789.

Ferreira, D., and J. Marshall, 2006: Formulation and implementation of a "residual-mean" ocean circulation model. *Ocean Modell.,* **13,** 86–107.

Fox-Kemper, B., 2004: Wind-driven barotropic gyre II: Effects of eddies and low interior viscosity. *J. Mar. Res.,* **62,** 195–232.

——, and J. Pedlosky, 2004: Wind-driven barotropic gyre I: Circulation control by eddy vorticity fluxes to an enhanced removal region. *J. Mar. Res.,* **62,** 169–193.

Gent, P. R., and J. C. McWilliams, 1990: Isopycnal mixing in ocean circulation models. *J. Phys. Oceanogr.,* **20,** 150–155.

Godfrey, J., 1989: A Sverdrup model of the depth-integrated flow for the World Ocean allowing for island circulations. *Geophys. Astrophys. Fluid Dyn.,* **45,** 89–112.

Green, J. S. A., 1970: Transfer properties of the large-scale eddies and the general circulation of the atmosphere. *Quart. J. Roy. Meteor. Soc.,* **96,** 157–185.

Harrison, D. E., and W. R. Holland, 1981: Regional eddy vorticity transport and the equilibrium vorticity budgets of a numerical model ocean circulation. *J. Phys. Oceanogr.,* **11,** 190–208.

---

[16] $\kappa \equiv \kappa_1 \mathbf{A}_{n,n}.$

Haynes, P., and M. E. McIntyre, 1987: On the evolution of vorticity and potential vorticity in the presence of diabatic heating and frictional or other forces. *J. Atmos. Sci.,* **44,** 828–841.

Held, I. M., 1975: Momentum transport by quasi-geostrophic eddies. *J. Atmos. Sci.,* **32,** 1494–1497.

Holland, W. R., and P. B. Rhines, 1980: An example of eddy-induced ocean circulation. *J. Phys. Oceanogr.,* **10,** 1010–1031.

Huang, R. X., 1987a: A three-layer model for the wind-driven circulation in a subtropical-subpolar basin. Part I: Model formulation and the subcritical state. *J. Phys. Oceanogr.,* **17,** 664–678.

——, 1987b: A three-layer model for the wind-driven circulation in a subtropical-subpolar basin. Part II: The supercritical and hypercritical states. *J. Phys. Oceanogr.,* **17,** 679–697.

——, 1988: A three-layer model for the wind-driven circulation in a subtropical-subpolar basin. Part III: Potential vorticity analysis. *J. Phys. Oceanogr.,* **18,** 739–752.

——, 1990: Matching a ventilated thermocline model with inertial western boundary currents. *J. Phys. Oceanogr.,* **20,** 1599–1607.

——, and G. R. Flierl, 1987: Two-layer models for the thermocline and current structure in subtropical/subpolar gyres. *J. Phys. Oceanogr.,* **17,** 872–884.

Johnson, G. C., and H. L. Bryden, 1989: On the size of the Antarctic Circumpolar Current. *Deep-Sea Res.,* **36A,** 39–53.

Killworth, P. D., 1997: On the parameterization of eddy transfer. Part I: Theory. *J. Mar. Res.,* **55,** 1171–1197.

Lee, M., 2002: Lagrangian motion of particles and tracers on isopycnals. *J. Phys. Oceanogr.,* **32,** 2086–2095.

Luyten, J. R., J. Pedlosky, and H. Stommel, 1983: The ventilated thermocline. *J. Phys. Oceanogr.,* **13,** 292–309.

Marshall, J. C., 1981: On the parameterization or geostrophic eddies in the ocean. *J. Phys. Oceanogr.,* **11,** 257–271.

——, and G. Nurser, 1992: Fluid dynamics of oceanic thermocline ventilation. *J. Phys. Oceanogr.,* **22,** 1315–1329.

McDougall, T. J., and P. C. McIntosh, 2001: The temporal-residual-mean velocity. Part II: Isopycnal interpretation and the tracer and momentum equations. *J. Phys. Oceanogr.,* **31,** 1222–1246.

Nadiga, B. T., 2008: Orientation of eddy fluxes in geostrophic turbulence. *Philos. Trans. Roy. Soc. London,* **A366,** 2491–2510.

Nurser, A. J. G., and R. G. Williams, 1990: Cooling Parsons' model of the separated Gulf Stream. *J. Phys. Oceanogr.,* **20,** 1974–1979.

Parsons, A. T., 1969: A two-layer model of gulf stream separation. *J. Fluid Mech.,* **39,** 511–528.

Pedlosky, J., 1987: On Parsons' model of the ventilated thermocline. *J. Phys. Oceanogr.,* **17,** 1571–1582.

Plumb, R. A., 1990: A nonacceleration theorem for transient quasigeostrophic eddies on a 3-dimensional time-mean flow. *J. Atmos. Sci.,* **47,** 1825–1836.

——, and R. Ferrari, 2005: Transformed Eulerian-mean theory. Part I: Nonquasigeostrophic theory for eddies on a zonal-mean flow. *J. Phys. Oceanogr.,* **35,** 165–174.

Radko, T., and J. Marshall, 2004: The leaky thermocline. *J. Phys. Oceanogr.,* **34,** 1648–1662.

Rhines, P. B., and W. R. Holland, 1979: A theoretical discussion of eddy-driven mean flows. *Dyn. Atmos. Oceans,* **3,** 289–325.

——, and W. R. Young, 1982a: Homogenization of potential vorticity in planetary gyres. *J. Fluid Mech.,* **122,** 347–367.

——, and ——, 1982b: A theory of the wind-driven circulation. 1. Mid-ocean gyres. *J. Mar. Res.,* **40** (Suppl.), 559–596.

Scott, R. B., and F. Wang, 2005: Direct evidence of an oceanic inverse kinetic energy cascade from satellite altimetry. *J. Phys. Oceanogr.,* **35,** 1650–1666.

Speich, S., H. A. Dijkstra, and M. Ghil, 1995: Successive bifurcations in a shallow-water model applied to the wind-driven ocean circulation. *Nonlinear Processes Geophys.,* **2,** 241–268.

Stammer, D., 1998: On eddy characteristics, eddy transports, and mean flow properties. *J. Phys. Oceanogr.,* **28,** 727–739.

Stommel, H. M., 1948: The westward intensification of wind-driven ocean currents. *Trans. Amer. Geophys. Union,* **29,** 202–206.

Sverdrup, H. U., 1947: Wind-driven currents in a baroclinic ocean; with application to the equatorial currents of the eastern Pacific. *Proc. Natl. Acad. Sci. USA,* **33,** 318–326.

Thompson, A. F., and W. R. Young, 2006: Scaling baroclinic eddy fluxes: Vortices and energy balance. *J. Phys. Oceanogr.,* **36,** 720–738.

Treguier, A. M., I. M. Held, and V. D. Larichev, 1997: Parameterization of quasigeostrophic eddies in primitive equation ocean models. *J. Phys. Oceanogr.,* **27,** 567–580.

Vallis, G. K., 2006: *Atmospheric and Oceanic Fluid Dynamics: Fundamentals and Large-Scale Circulation.* Cambridge University Press, 745 pp.

Veronis, G., 1973: Model of world ocean circulation. Part I: Wind-driven, two-layer. *J. Mar. Res.,* **31,** 228–288.

——, 1976: Model of world ocean circulation. Part II: Thermally-driven, two-layer. *J. Mar. Res.,* **34,** 199–216.

——, 1978: Model of world ocean circulation. Part III: Thermally and wind driven. *J. Mar. Res.,* **36,** 1–44.

Wardle, R., and J. Marshall, 2000: Representation of eddies in primitive equation models by a PV flux. *J. Phys. Oceanogr.,* **30,** 2481–2503.

Warren, B., J. LaCasce, and P. Robbins, 1996: On the obscurantist physics of "form drag" in theorizing about the circumpolar current. *J. Phys. Oceanogr.,* **26,** 2297–2301.